University of Campinas
Institute of Physics Gleb Wataghin

Physical Principles of Neuroimaging Techniques

Sérgio Luiz Novi Junior

Prof. Dr. Rickson C. Mesquita

Campinas 2016

Dedico este trabalho à minha avó, Nair Novi.

Abstract

Thanks to powerful and advanced techniques based on physics, we are capable to extract information from the human brain with high temporal and spatial resolution. Among several techniques capable to image the brain, magnetic resonance imaging (MRI) and near-infrared spectroscopy (NIRS) are highlighted due to their intrinsic noninvasiveness. In other words, with any of these techniques, one can estimate neural activity without damaging the cerebral tissue. In this work, we extensively discuss the most important physical principles behind each technique, MRI and NIRS.

Contents

List of Figures

Chapter 1

Introduction

The human brain is probably the most complex system at hand. It is optimized, being capable to perform difficult tasks quickly and very effective. Understanding its mechanisms is crucial to improve treatments of neurological diseases, such as epilepsy and Alzheimer [2, 3]. Thanks to powerful and advanced techniques grounded on physics, chemistry and biology, we are capable to extract information from the human brain with high temporal and spatial resolution. Among several neuroimaging techniques, electroencephalography (EEG), magnetic resonance imaging (MRI) and near-infrared spectroscopy (NIRS) are highlighted due to their intrinsic noninvasiveness, ease of use and reliability.

EEG was developed more than one century ago, being the first technique capable to image the brain. The English physician Richard Caton (1842-1926) is pointed to be the first one to successfully employ EEG to measure electrical activity of the brain in 1875. Cato's studies were performed in cats, monkeys and rabbits. Although Berger showed in the 1920s that the EEG could be recorded from the human scalp, the acceptance of EEG as a method to investigate brain function in healthy and diseased brains only started in 1934. At that time, Adrian and Mathews showed that electrical signals measured in the occipital lobe in man were reliable and not generated due to residual artefacts [4].

The EEG signal consists in measuring the summed of activities from populations of neurons. Neurons are cells that produce electrical and magnetic fields when they are activated. The electrical fields can be recorded by displacing electrodes right in the region of interest, inside the brain, in the surface of the cerebral cortex or in the scalp. In noninvasiveness EEG experiments, the electrodes are generally placed in the scalp of volunteers; thereby the acquired signal lacks spatial resolution. It is the main disadvantage of the EEG technique.

In the beginning of 1990, MRI started to become the principal neuroimaging technique [5]. It had an exponential growth since its invention. The growth of MRI can be associated to the robustness, versatile and high spatial resolution of this technique. MRI was primarily used to anatomically investigate the structure of the brain based on density of protons mainly from water and fat molecules. Succinctly, its mechanisms consist on an external and constant magnetic field to break the degeneracy of the hydrogen atoms then applying a sequence of radio frequency (RF) electromagnetic waves to extract information from the brain structure. There are several radio frequency pulse sequences available, which are sensible to different aspects of the healthy and diseased brain tissue. For example, to construct a high contrast between gray matter and white matter, T-1 weighted sequence can be successfully employed. This sequence is a combination of a short time repetition and short echo time. Time repetition refers to the time between successive RF pulses, and echo time stands to the time in which the electrical signal induced by the spinning protons is measured.

More recently, near-infrared spectroscopy has appeared as a promising technique to image the brain function [6, 7]. In the NIRS technique, low level lights in the NIR spectra (from 650 to 900nm) are used to estimate optical absorption changes in the human brain. This can be acquired by displacing optodes in the heads surface non-invasively. The optodes emit and receive light, recording light intensity variations. In the NIR spectra window, light is greater scatter than absorber by the biological tissue. Therefore, the light can penetrate up to the cerebral cortex, 5-10 mm in the brain, then come back to the head surface, carrying optical information from the brain [8]. The optical measurements from different wavelengths can be used to estimate concentrations changes of oxy-hemoglobin (HbO) and deoxy-hemoglobin (HbR) due to their differences regarding absorption of light. HbO and HbR concentration changes are related to local brain activity, thereby it is possible to image the brain function.

In the present work, we aim to describe the physical principles behind magnetic resonance imaging and near-infrared spectroscopy. Although the content is developed for being understood for any student in the last year of the undergraduate physics course, it should provide useful knowledge for new researchers to the neuroscience field. In Chapter 2, we start by briefly discussing the concept of nuclear spin then we investigate the interaction of spins with an external magnetic field. Next, we model the interaction of a macroscopic ensemble of protons subjected to an external magnetic field and being excited by electromagnetic waves in the radio frequency. To do so, we considered that the system of protons were in contact with a thermal bath

so that we could use the canonical ensemble combined with quantum mechanics. In the end of chapter 2, we used a classical approach by defining a net magnetization. As a result, we could derive the well-known phenomenological Bloch equations. Next, we investigated the interaction of the system under the influence of RF fields, using the Bloch equations.

In chapter 3, we studied the physical principles of near-infrared light propagation through the biological tissue. We started by discussing basic yet crucial concepts of light-matter interaction, scattering and absorption. Next, we used the Radiative Transport (RT) Theory as an approximation to the Maxwell's equations for describing NIR light propagation. For doing that, we defined a physical quantity called radiance so that we could derive the well-known Radiative Transport equation (RTE). Latter, we expanded the RTE in spherical harmonics to derive a photon diffusive approximation, which provides us valuable physical insights regarding NIR light propagation. In the end of the chapter, we summarized all assumptions behind each approximation that we had to do to derive the photon diffusive approximation as well discussed under which circumstances our results are valid.

Chapter 2

Nuclear Magnetic Resonance Imaging

In this chapter, we study the physical principles behind nuclear magnetic resonance imaging. We start by introducing the concept of nuclear spin and defining the Hamiltonian of a proton under the influence of a constant external magnetic field. Next, we model the interaction of a macroscopic system of protons under the influence of a constant external magnetic field and being excited by electromagnetic waves in the radio frequency. In the end, we could derive the phenomenological Bloch equations, using a classical approach.

2.1 Principles of Nuclear Magnetic Resonance

Nuclear magnetic resonance (NMR) is a quantum phenomenon related to the total spin of a nucleus. All nuclei present the intrinsic property of "nuclear spin", which is the sum of the orbital spin and the angular momentum of all particles that compose the nucleus, denoted by $\mathbf{J}$. $\mathbf{J}$ has unity of $\hbar$ in which $\hbar$ is the Planck constant over 2π. We can define a dimensionless angular momentum operator, I, by dividing $\mathbf{J}$ by $\hbar$:

$$\mathbf{J} = \hbar\mathbf{I} \rightarrow \mathbf{I} = \frac{\mathbf{J}}{\hbar}. \tag{2.1}$$

Due to the nuclear charge and nuclear spin, nuclei have a magnetic momentum, $\boldsymbol{\mu}$, which is proportional to $\mathbf{J}$,

$$\boldsymbol{\mu} = \gamma\mathbf{J} = \gamma\hbar\mathbf{I}; \tag{2.2}$$

where γ is the Lande factor.

In the presence of a external magnetic field, $\mathbf{B}$, the interaction between the nuclear spin and the external field is given by the Hamiltonian:

$$H = -\boldsymbol{\mu} \cdot \mathbf{B} \rightarrow H = -\gamma\hbar(\mathbf{I} \cdot \mathbf{B}). \tag{2.3}$$

Defining the external magnetic field as a constant and only with component in the $\hat{k}$ direction, we have $\mathbf{B} = B_0\hat{k}$ and, consequently,

$$H = -\gamma\hbar I_z B_0 \rightarrow \text{ Energy} = E = -\gamma\hbar B_0 m_z; \tag{2.4}$$

where I_z is the projection of I in the $\hat{z}$ direction. The eigenvalues m_z vary such that $m_z = -I_z, -I_z + 1, ..., I_z - 1, I_z$. In the present work, we will deal only with the proton, which has nuclear spin 1/2. Considering protons, all possible values for m_z are $1/2$ and $-1/2$. In addition, I will denote by $|\alpha\rangle$ and $|\beta\rangle$ the eigenstates with spins $+1/2$ and $-1/2$, respectivelly. Hence, the energy of the states $|\alpha\rangle$ and $|\beta\rangle$ are given by:

$$E_\alpha = -\frac{1}{2}\gamma\hbar B_0,$$

$$E_\beta = +\frac{1}{2}\gamma\hbar B_0. \tag{2.5}$$

Thus, the fundamental and excited states corresponds respectivelly to the kets $|\alpha\rangle$ and $|\beta\rangle$. The energy difference between the states $|\alpha\rangle$ and $|\beta\rangle$ is given by $E_\beta - E_\alpha = \Delta E = \gamma\hbar B_0$. Note that the energy difference is linearly proportional to the magnitude of the external magnetic field, $\mathbf{B}$ (Figure 2.1).

A proton in the $|\alpha\rangle$ state can be excited to the $|\beta\rangle$ state by absorbing an electromagnetic wave, or a photon, in the radio frequency (rf). The absorption will occur under two conditions. First, the electromagnetic wave frequency, ν, should match the energy difference between the two allowed states. Second, the oscillating vector field from the rf wave should be perpendicular to the external magnetic field $\mathbf{B}$ then

$$E_{photon} = \gamma\hbar B_0, \tag{2.6}$$

but $E_{photon} = h\nu$ and $\nu = \frac{\omega}{2\pi}$, thus:

$$\nu = \frac{\gamma B_0}{2\pi}. \tag{2.7}$$

$$\omega = \gamma B_0. \tag{2.8}$$

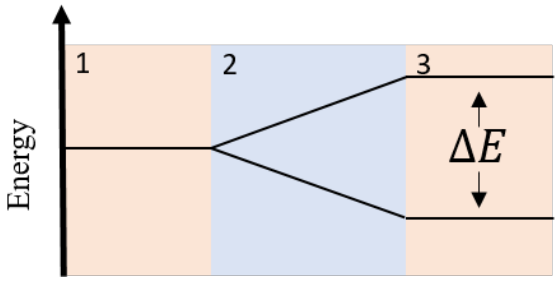

Figure 2.1: Energy from the interaction of proton with an external magnetic field. In region one,$B = 0$, the energy interaction is zero because there is no external magnetic field. As a consequency, spins in the up and down directions have same energy. In region two, the magnitude of the external magnetic field is increased linearly, which splits the two spin states and increases proportionally to the external field the energy gap between them. In the third region, the external magnetic field is constant and different from zero, thereby there is a constant energy gap.

From equations 2.7 and 2.8, we can conclude that it is possible to observe nuclear absorption by resonance by varying the frequency of the rf waves or by varying the intensity of the external magnetic field. In pratice, the choice depends on what is more convinient to the scientist. To characterize a solid, one usually works with a fixed frequency ν and varies the external magnetic field around the resonance point. We should also realize that the NMR technique is only sensitive to the protons on the fundamental states. We are not capable to excite protons in the highest level of energy via resonance by rf waves.

2.2 Thermal Equilibrium and Spin Relaxation Time

In this section, we will investigate consequences of applying an external magnetic field $\mathbf{B} = B_0\hat{k}$ to a macroscopic spin system. We approach this problem by using the canonical emsemble, which means that we assumed the system is in thermal equilibrium with a heat bath at some fixed temperature. In this ensemble, we can use the Boltzmann's distribution, which states that the number of microstates decays exponentially with the increase of the energy associated with each state, i.e.:

$$\text{Number of states} = A\exp(-E/(\kappa T)), \tag{2.9}$$

where κ is the Bolztmann constant, T is the temperature of the system, and A is a constant of normalization.

Using equation 2.9, we can calculate the ratio between the number of protons in the $|\alpha\rangle$ and $|\beta\rangle$ states, which is given by:

$\frac{N_\alpha}{N_\beta} = \frac{A\exp(-E_\alpha/(\kappa T))}{A\exp(-E_\beta/(\kappa T))} = \exp\,(\frac{E_\beta - E_\alpha}{\kappa T})$. Therefore,

$$\frac{N_\alpha}{N_\beta} = \exp(\frac{\gamma\hbar B_0}{\kappa T}). \tag{2.10}$$

Equation 2.10 is by itself a very interesting result. In the last section, I argued that nuclear magnetic experiments are only sensitive to protons in the fundamental states. Note that if $\mathbf{B}$ is increased, the ratio N_α/N_β also increases. However, the total number of spins, $N = N_\alpha + N_\beta$, is constant. Thus, there is an increasement in the number of spins in the lower energy state, implying that there are more spins to be flipped. This relation is the only mechanism capable to explain why stronger external magnetic fields provide nuclear magnetic resonance images with a higher spatial resolution.

Let us verify the effect of aplying an oscilatting magnetic field (rf field) to the spin system. To do so, I will use a result from time-dependent perturbation theory. Suppose that a pertubation $V(t)$ is applied to a system with discrete energy levels, the rate change from one level to the other is given by:

$$P_{ab} = \frac{2\pi}{\hbar}|\,\langle b|V(t)|a\rangle\,|^2\delta(E_b - E_a - h\nu), \tag{2.11}$$

where P_{ab} is the probability of transition from state a to state b, measured by the number of transitions per second, and δ is the Dirac delta function. The delta functions impose that there are no transitions if $h\nu$ is different from $E_b - E_a$. Although we are supposing that absorption only occurs for a specific frequency ν, we will discuss later that it is not entirelly correct. Due to the energy-time uncertainty principle, absorption occurs for a frequency range. The most important point for us regarding equation 2.11 is that $|\,\langle b|V(t)|a\rangle\,|^2$ is equal to $|\,\langle a|V(t)|b\rangle\,|^2$, which implies that $P_{ab} = P_{ba}$. We will call transitions that were caused by the rf filed by stimulated transitions, and transitions that occured because of other reasons by spontaneous. Therefore, The rate change in the number of protons in the fundamental state can be modeled by:

$$\frac{dN_\alpha}{dt} = N_\beta P_{\beta\alpha} - N_\alpha P_{\alpha\beta} = P(N_\beta - N_\alpha), \tag{2.12}$$

where the first term accounts for the spins that decay from the excited state to the fundamental state, the second term accounts for the spins that were excited from the fundamental state to the excited one, and $P \equiv P_{\alpha\beta} = P_{\beta\alpha}$.

Changing variables in equation 2.12 of $n = N_\alpha - N_\beta$ and substituiting $N_\alpha = \frac{1}{2}(N+n)$ and $N_\beta = \frac{1}{2}(N-n)$. We have:

$$\frac{dN_\alpha}{dt} = \frac{1}{2}\frac{dn}{dt} = -Pn \rightarrow \frac{dn}{dt} = -2Pn. \tag{2.13}$$

Therefore,

$$n(t) = n(0)e^{-2Pt}, \tag{2.14}$$

where $n(0)$ is the difference in the states in $t = 0$. Another quantity of interest is the rate of absorption of energy from the radiation field, $\frac{dE}{dt}$:

$$E = E_{system} = N_\alpha E_\alpha + N_\beta E_\beta \rightarrow \frac{dE}{dt} =$$

$$= \frac{dN_\alpha}{dt}E_\alpha + \frac{dN_\beta}{dt}E_\beta,$$

but $\frac{dN_\alpha}{dt}$ is given by equation 2.12 and $\frac{dN_\beta}{dt} = -\frac{dN_\alpha}{dt}$. Therefore,

$$\frac{dE}{dt} = N_\alpha P_{\alpha\beta}(E_\beta - E_\alpha) + N_\beta P_{\beta\alpha}(E_\alpha - E_\beta) = nP\Delta E. \tag{2.15}$$

Equation 2.14 tells us that after a long time that the rf field perturbates the system of spins, the difference between the population of spins on the excited and fundamental states will become zero, $n(t) \rightarrow 0$. This configuration is called *saturation*. It is characterized by the absence of resonance absorption.

In addition, we should note that the developed model to the spin dynamics lacks some other interactions. Note that in the presence of the external magnetic field, we used the Boltzmann's distribution to infer that there were a population diference in the system, $N_\alpha > N_\beta$. However, in the absence of the external magnetic field N_α should be equal to N_β via the same distribution. Therefore, there are other interactions between the nuclei and their surroudings which cause the spin orientation to change. The excess of magnetic energy is converted to other degrees of freedom. This nonradiative transitions are called *spin-lattice relaxation*. The physical key behind spin-lattice relaxation is that the whole system of spins is in thermal equilibrium in which the probabilities of spontaneous spin transitions are not equal as it were for the rf field.

To properly model the spin transition dynamics, we should also consider the relaxation probabilities $W_{\alpha\beta} \equiv W_{\alpha\rightarrow\beta}$ and $W_{\beta\alpha} \equiv W_{\beta\rightarrow\alpha}$ due to the interaction between the nuclei and their surroundings. Let us considere the case without the rf field:

$$\frac{dN_\alpha}{dt} = N_\beta W_{\beta\alpha} - N_\alpha W_{\alpha\beta}. \tag{2.16}$$

At thermal equilibrium, we should have $\frac{dN_\alpha}{dt} = 0 \rightarrow N_\beta^0/N_\alpha^0 = W_{\alpha\beta}/W_{\beta\alpha}$. Changing again variables to $n = N_\alpha - N_\beta$ and $N = N_\alpha + N_\beta$:

$$\frac{dn}{dt} = -n(W_{\beta\alpha} + W_{\alpha\beta}) + N(W_{\beta\alpha} - W_{\alpha\beta}) \tag{2.17}$$

that may be written as:

$$\frac{dn}{dt} = -\frac{(n - n_0)}{T_1}; \tag{2.18}$$

where n_0 ($n_0 = N[(W_{\beta\alpha} - W_{\alpha\beta})/(W_{\beta\alpha} + W_{\alpha\beta})]$) is the population difference at thermal equilibrium ($N_\alpha^0 - N_\beta^0$), and $1/T_1$ is equal to $W_{\alpha\beta} + W_{\beta\alpha}$. Note that T_1 has dimension of time, and it is called the *spin-lattice relaxation time*. T_1 provides an idea of how long it takes for the lattice to approach thermal equilibrium. Different systems can have different spin-lattice relation time. For example, cerebral cortex, or gray matter, presents T_1 aprroximattely $950ms$ and white matter $600ms$, while blood has T_1 around $1200ms$.

We are now able to combine the effects of the rf field and the spin relaxation time by combining equations 2.13 and 2.18:

$$\frac{dn}{dt} = -2Pn - \frac{(n - n_0)}{T_1}. \tag{2.19}$$

At equilibrium, $dn/dt = 0$, the population difference will be given by:

$$n = \frac{n_0}{1 + 2PT_1}, \tag{2.20}$$

which implies that the rate of absorption of rf energy (recall equation 2.15) is given by:

$$\frac{dE}{dt} = n_0 \Delta E \frac{P}{1 + 2PT_1}, \tag{2.21}$$

this equation indicates that if T_1 is larger, the system will easily saturate.

To investigate the dynamics of the macroscopic system of spins, we basically considered that the width and shape of the absorption line could be represented by a δ function. However, it is a quite unreallistic approach. First of all, there is an uncertatinty in the energy that can be absorbed by the spin in the process of resonance. From the uncentainty principle of time and energy, we know that:

$$\Delta t \Delta E \geq \hbar/2 \rightarrow \Delta t(h\Delta\nu) = \hbar/2 \rightarrow \Delta t \Delta\nu \sim 1$$

.

Besides, there are other mechanisms that affect the relative energies of the spin levels. These mechanisms are characterized by a relaxation time T_2, which is known as the *transverse relaxation time*. The transverse relaxation time is closely linked to the spin-lattice relaxation time due to the fact that they are both related to similar interactions between the spin and their surroundings. To take in account the transverse relaxation time, we should replace the Delta distribution function by another one such as the Lorentzian and Gaussian function. One detailed approach to resonance absorption can be found on [9] (chapter 13 and section C).

2.3 Bloch Equations

In this section, we will model the interaction of spins with their surroungings in the presence of an external field by the phenomenological Bloch's equations [10]. In this approach, we should use the concept of a net magnetization vector, $\mathbf{M}(\mathbf{r}, t)$ that is the sum of the individual magnetic moments of all protons inside a fixed volume V.

Suppose that there were an external magnetic field for some period of time then the external field is turned to zero. Right after turning off the system, the configuration is given by N_α protons in the $|\alpha\rangle$ state and N_β in the $|\beta\rangle$ state. Therefore, the magnetization inside the volume is given by:

$$M_z = \gamma\hbar(N_\alpha - N_\beta) = \gamma\hbar n. \tag{2.22}$$

However, due to the protons interactions with their surroundings, the magnetization will decrease exponentially to zero, equation 2.18. Differentiating the magnetization in respect to time, we have:

$$\frac{dM_z}{dt} = \gamma\hbar\frac{dn}{dt} = -\gamma\hbar\frac{n}{T_1} = -\frac{M_z}{T_1}. \tag{2.23}$$

Note that there is no difference between the z, x, and the y direction. Hence,

$$\begin{aligned}
\frac{dM_z}{dt} &= -\frac{M_z}{T_1};\\
\frac{dM_x}{dt} &= -\frac{M_x}{T_1};\\
\frac{dM_y}{dt} &= -\frac{M_y}{T_1}.
\end{aligned}$$

When the external magnetic field is turned on such that $B = B_0\hat{z}$, z, x, and y directions are no longer similar and the magnetization in the z direction does not

tend to zero anymore. However, the magnetization is still given by $M_z = \gamma\hbar n$ then according to equation 2.18, we should have:

$$\frac{dM_z}{dt} = -\frac{M_z(t) - M_z(0)}{T_1}. \tag{2.24}$$

The magnetization in the other directions will still decay exponentially to zero, but the spin relaxation time from them do not have necessarily to be equal to the one from the z direction in which the external field has been applied. Thus,

$$\begin{aligned} \frac{dM_x}{dt} &= -\frac{M_x}{T_2} \\ \frac{dM_y}{dt} &= -\frac{M_y}{T_2} \end{aligned} \tag{2.25}$$

To finish the whole description, we should add the contribution from the spin angular momentum of the entire volume V. Here, we assume that the angular momentum of each nucleus obeys the classical mechanics. The torque in each magnetic moment due to the external magnetic field is given by:

$$\vec{\tau} = \vec{\mu} \times \mathbf{B}, \tag{2.26}$$

but $\frac{d\mathbf{L}}{dt} = \vec{\tau}$ then

$$\frac{d\mathbf{L}}{dt} = \frac{d(\hbar\mathbf{I})}{dt} = \vec{\mu} \times \mathbf{B}. \tag{2.27}$$

Multiplying both sides by γ:

$$\frac{d\vec{\mu}}{dt} = \gamma\vec{\mu} \times \mathbf{B}. \tag{2.28}$$

The total magnetization $\mathbf{M}$ is the sum of all magnetic moment within a fixed volume V, thereby $\mathbf{M}$ behaves similarly to each magnetic moment:

$$\frac{d\mathbf{M}}{dt} = \gamma\mathbf{M} \times \mathbf{B}, \tag{2.29}$$

which implies that:

$$\begin{aligned} \frac{dM_x}{dt} &= \omega_0 M_y \\ \frac{dM_y}{dt} &= -\omega_0 M_x \\ \frac{dM_z}{dt} &= 0 \end{aligned} \tag{2.30}$$

in which ω_0 is the nuclear resonance frequency, (γB_0), which is also known as the Larmor frequency. Combining equations 2.24, 2.25, and 2.30, we find the Bloch equations:

$$\begin{aligned}
\frac{dM_x}{dt} &= \omega_0 M_y - \frac{M_x}{T_2} \\
\frac{dM_y}{dt} &= -\omega_0 M_x - \frac{M_y}{T_2} \\
\frac{dM_z}{dt} &= -\frac{M_z(t) - M_z(0)}{T_1}.
\end{aligned} \tag{2.31}$$

Therefore, on one hand, the net magnetization vector performs a damped precesion in which its longitudinal component M_z relaxes to its equilibrium M_0 with a decay characteristic time T_1. On the other hand, the transverse components of M decay to zero with a time T_2.

2.3.1 Radio Frequency Field

With the Bloch's equations, we can investigate the macroscopic result of applying an rf oscillating field to the sample of spins. For simplicity, I will solve this problem for a rotating magnetic filed B_1. However, note that a field of strength $2B_1 \cos \omega t$ in the x direction can be understood as the sum of two counter-rotating fields, $(B_1 \cos \omega t, -B_1 \sin \omega t, 0)$ and $(B_1 \cos \omega t, +B_1 \sin \omega t, 0)$. Regarding these two rotating magnetic fields, only the first one can be in resonance with the nuclear spins because the external steady magnetic field B_0 is pointed to the z direction. The other has no significant effect. Therefore, a rotating field $(B_1 \cos \omega t, -B_1 \sin \omega t, 0)$ is approximately equal to an oscillating field of strength $2B_1$.

If we apply a radio frequency field B_1 that oscillates in the Larmor frequency, the net magnetization will feel a torque, which is synchronized to the free precession of the net magnetization, thereby a large oscillating magnetic field will be induced in the sampple. Instead, a field which oscillates at other frequencies will have only small effects on the sample. Therefore, to investigate the resonance in detail, let us apply a circurlarly polarized rf filed $\mathbf{B_1}$ which rotates clockwise in the xy plane with angular velocity ω.

$$\mathbf{B_1} = B_1(\hat{x} \cos \omega t - \hat{y} sin(\omega t)). \tag{2.32}$$

Hence, we have to add in the Bloch's equations a new torque because of the interaction between $\mathbf{B_1}$ and the magnetization vector:

$$\frac{d\mathbf{M}}{dt} = \gamma\mathbf{M} \times \mathbf{B} + \gamma\mathbf{M} \times \mathbf{B_1} - \frac{\hat{x}M_x + \hat{y}M_y}{T_2} - \frac{\hat{z}(M_z - M_0)}{T_1}. \tag{2.33}$$

We can define a new coordinate system that rotates with $\mathbf{B_1}$ at angular velocity ω. In the new system, S', we set x' on the direction of $\mathbf{B_1}$, z' on the direction of $\mathbf{B}$, and y' such that $x' \times y' = z'$. We also define u and v to be the transverse components of the magnetic moment along the x' and y' directions, respectively. Thus,

$$\mathbf{M}' = u\hat{x}' + v\hat{y}' + M_z\hat{k}'.$$

$$\mathbf{B_1}' = B_1\hat{x}'.$$

$$\vec{\omega}' = -\omega\hat{k}'.$$

In respect to S' system, the change rate of $\mathbf{M}'$ is given by:

$$\frac{d\mathbf{M}'}{dt} = \frac{du}{dt}\hat{x}' + \frac{dv}{dt}\hat{y}' + \frac{dM_z}{dt}\hat{k}'.$$

However, for an observer in the fixed system, the x' axis changes with time such that:

$$x' = \hat{x}cos(\omega t) - \hat{y}\sin\omega t \rightarrow \frac{dx'}{dt} = -\hat{x}sin(\omega t)\omega - \hat{y}\cos(\omega t)\omega.$$

The magnetization would be:

$$\mathbf{M} = u\hat{x}' + v\hat{y}' + M_z\hat{k}', \tag{2.34}$$

but the axis are rotating, so:

$$\frac{d\mathbf{M}}{dt} = \frac{du}{dt}\hat{x}' + \frac{dv}{dt}\hat{y}' + \frac{dM_z}{dt}\hat{k}' + \frac{dx'}{dt}u + \frac{dy'}{dt}v, \tag{2.35}$$

which leads to:

$$\frac{d\mathbf{M}}{dt} = \frac{d\mathbf{M}'}{dt} + \vec{\omega}' \times \mathbf{M}'. \tag{2.36}$$

Assuming that at time $t = 0$, the systems S and S' coincide, and using equations 2.33 and 2.36, we should have:

$$\frac{d\mathbf{M}'}{dt} + \vec{\omega}' \times \mathbf{M}' = \gamma\mathbf{M}' \times \mathbf{B}' + \gamma\mathbf{M}' \times \mathbf{B_1}' - \frac{\hat{x}'M_x + \hat{y}'M_y}{T_2} - \frac{\hat{z}'(M_z - M_0)}{T_1}. \tag{2.37}$$

The separation of components yields:

$$\frac{du}{dt} = (\omega_0 - \omega)v - \frac{u}{T_2};$$

$$\frac{dv}{dt} = -(\omega_0 - \omega)u + \gamma B_1 M_z - \frac{v}{T_2}; \tag{2.38}$$

$$\frac{dM_z}{dt} = -\gamma B_1 v - \frac{M_z - M_0}{T_1}.$$

After the rf field has been on for a long time, the spin precession reaches a stationary state such that the solutions of equations 2.38 are given by:

$$u = M_0 \frac{\gamma B_1 T_2^2(\omega_0 - \omega)}{1 + T_2^2(\omega_0 - \omega)^2 + \gamma^2 B_1^2 T_1 T_2};$$

$$v = M_0 \frac{\gamma B_1 T_2}{1 + T_2^2(\omega_0 - \omega)^2 + \gamma B_1^2 T_1 T_2}; \tag{2.39}$$

$$M_z = M_0 \frac{1 + T_2^2(\omega_0 - \omega)^2}{1 + T_2^2(\omega_0 - \omega)^2 + \gamma B_1^2 T_1 T_2}.$$

In the beginning of this section, we discussed that the solution for an oscillating field is equivalent to a rotating field with strength of $2B_1$. From now on, we will use the oscillating magnetic field which is basically $(2B_1 \cos(\omega t), 0, 0)$. The components of the oscillating external field and the net magnetization in the fixed coordinates become:

$$B_{1x} = 2B_1 \cos(\omega t).$$

$$M_x = u \cos(\omega t) + v \sin(\omega t). \tag{2.40}$$

Therefore, note that u is component of M that oscillates in phase with $\mathbf{H_1}$, while v presents a phase delay of $\frac{\pi}{2}$. Bloch described this phase shift by introducing a complex magnetic suceptibility $\chi(\omega)$. In this perspective, H_{1x} and M_x are descibed respectively as $2H_1 exp(-i\omega t)$ and $2H_1\chi(\omega)exp(-i\omega t)$. $\chi(\omega)$ is equal to $\chi(\omega)' + i\chi(\omega)''$, and the real magnetic moment is given by the real part of $2H_1\chi(\omega)exp(-i\omega t)$, which implies that u and v are proportional to $\chi'(\omega)$ $\chi''(\omega)$:

$$M_x = H_1[\chi(\omega)e^{-i\omega t} + \chi^*(\omega)e^{i\omega t}] =$$

$$= 2H_1\chi'(\omega)\cos\omega t + 2H_1\chi''(\omega)\sin\omega t. \tag{2.41}$$

Comparing equation 2.40, 2.39 and 2.41 and writting M_0 as $\chi_0 H_0$, we can express the sample's susceptibilities as:

$$\chi(\omega)' = \frac{1}{2}\chi_0\omega_0 \frac{T_2^2(\omega_0 - \omega)}{1 + T_2^2(\omega_0 - \omega)^2 + \gamma^2 B_1^2 T_1 T_2};$$

$$\chi(\omega)'' = \frac{1}{2}\chi_0\omega_0 \frac{T_2}{1 + T_2^2(\omega_0 - \omega)^2 + \gamma^2 B_1^2 T_1 T_2}. \tag{2.42}$$

By holding B_1 constant, we can investigate the behavior of $\chi(\omega)'$ $\chi(\omega)''$ as function of $(\omega - \omega_0)T_2$ in units of $\frac{1}{2}\chi_0\omega_0 T_2$. From figure 2.2, we note that at the resonance frequency, ω_0, $\chi(\omega)''$ becomes very large and $\chi(\omega)'$ changes sign. However, far from the resonance point, $\chi(\omega)''$ approaches zero very quickly. At high frequencies, $\chi(\omega)'$ is negative what makes the $\mathbf{M}$ to be π (out of phase). The rotating H_1 produces a torque on the magnetic moments of the spins with magnitude vH_1 in the $\hat{z}$ direction. It does work on the precessing rate spins at a rate $\omega v H_1$. Comparing again equations 2.40 and 2.41, the average power absorbed by the sample of spins is given by:

$$\frac{dE}{dt} = 2\omega H_1^2 \chi(\omega)''. \tag{2.43}$$

Therefore, at the resonance frequency, there is a strong absorption of energy since $\chi(\omega)''$ increases significantly.

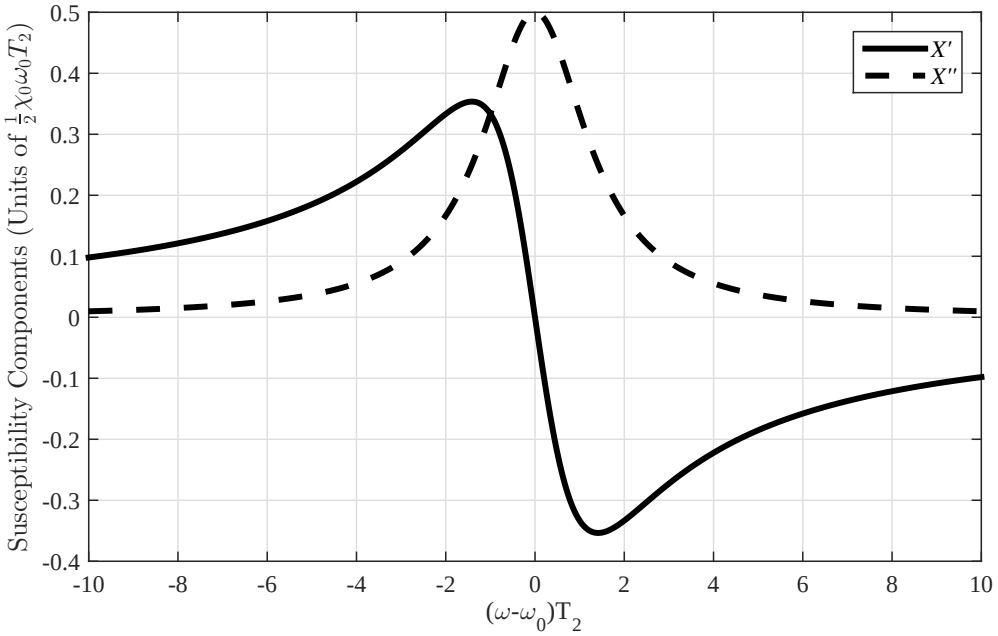

Figure 2.2: Behavior of the susceptibilities as function of $(\omega - \omega_0)T_2$.

Chapter 3

Near-Infrared Spectroscopy

In this chapter, we investigate the physical principles behind NIR light propagation through the biological tissue. First, we introduce basic concepts of light-matter interaction, scattering and absorption. Next, we use the Radiative Transport Theory as an approximation to the Maxwell's equations for describing NIR light propagation through the biological tissue, resulting in the Radiative Transport Equation. To provide valuable physical insights regarding NIR light propagation, we derive a photon diffusive approximation by expanding the Radiative Transport Equation in spherical harmonics. In the end, we discuss the validity of our findings.

3.1 Absorption and Scattering

In order to properly extract and interpret optical information from a medium, one must be familiar with two basic concepts regarding light-matter interaction: scattering and absorption.

Scattering is related to the change in the direction of the light inside a medium. In this process, photons are absorbed by molecules from the tissue then they are re-emitted. The re-emitted photon may have the same energy and momentum as the incident photon, same energy and different momentum or different energy and momentum. Using low power sources in the NIR spectra, scattered photons by the biological tissue predominantly have the same energy as the incident photons. Therefore, we can restrict ourselves to study only elastic scattering, i.e. scattering in which energy is conserved. Elastic scattering can provide structural information about cells and surrounding fluids because it is originated due to spatial differences on the scale of the light wavelength, $0.6\mu m$. Tissue presents several regions of greater and lesser density on a length scale comparable to the NIR wavelengths (600-950nm). For exam-

(a) Hydrogen Spectrum

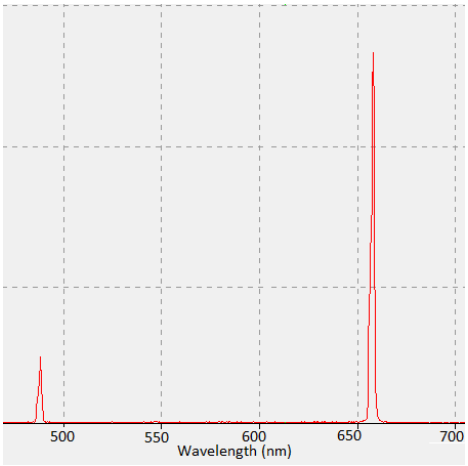

(b) Absorption Coefficient

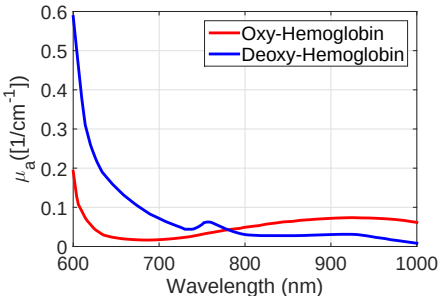

Figure 3.1: The hydrogen spectrum has only very specific wavelengths in which absorption is observed, while the absorption coefficients for oxy- and deoxy-hemoglobins are different from zero in a basically continuum spectrum. Data for 3.1a were acquired in the learning experimental physics lab from the University of Campinas, and data for 3.1b were extracted from http://omlc.org/spectra/.

ple, the size of a red blood cell is about $7.8\mu m$; thereby this medium is very scattering to the NIR light.

Absorption refers to the process in which electromagnetic energy is converted into internal energy of the medium, usually thermal energy. Typically, in the undergraduate physics courses, students work only with interactions between light and electrons or atoms. In those cases, the frequencies in which one can observe absorption events are very limited. To observe absorption, the incident photon energy should basically match the energy difference between the electronic states of a bound electron. These energy differences are discrete, limiting the interactions to specific wavelengths, Figure 3.1a.

However, in the biological tissue, an incident photon to be absorbed may also match the energy differences in the rotational or vibrational modes of one of the molecules that constitute the medium. These energy gaps depend on the temperature of the medium, making the absorption spectrum basically continuum due to thermal fluctuations. In the NIR spectra, the main absorbing constituents of the tissue are oxy-hemoglobin, deoxy-hemoglobin, water and lipid, figure 3.1b b). With measurements of absorption using different wavelengths, it is possible to extract concentrations of each one of these chromophores.

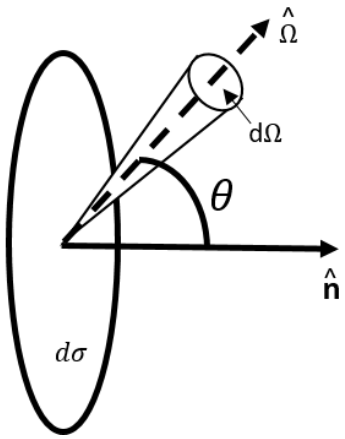

Figure 3.2: Light radiance traveling in the direction $\hat{\mathbf{\Omega}}$. The amount of radiant power crossing an element of area $d\sigma$ is given by $L\cos\theta d\sigma d\Omega$ in which θ is the angle between $\hat{\mathbf{\Omega}}$ and the vector $\hat{\mathbf{n}}$, normal to the infinitesimal area $d\sigma$. This figure is adapted from [1].

3.2 Radiative Transport Equation

Light propagation in the biological tissue could be modeled by using directly the Maxwell's equations. To do so, we would have to account for every interaction of the light with the medium, which makes this approach not viable. One alternative method is to use the Radiative Transport (RT) Theory as an approximation to Maxwell's equations for describing light propagation through tissue [11, 12]. A very formal and detailed derivation of the Radiative Transport Equation (RTE) can be found on [13].

The most important physical quantity in the RT theory is the light radiance, $L(\mathbf{r}, \hat{\mathbf{\Omega}}, t, \lambda)$ [14]. The units of L are $[Wcm^{-2}sr^{-1}]$, i.e. L is basically the light power per unit area per unit solid angle traveling in the $\hat{\mathbf{\Omega}}$ direction at position $\mathbf{r}$ and time t. With L, we can directly express the amount of radiant power, $W(\hat{\mathbf{\Omega}})$, crossing an element of area $d\sigma$ in direction within an element of solid angle $d\Omega$, $d\Omega = \sin\theta d\theta d\phi$ (Figure 3.2):

$$W(\hat{\mathbf{\Omega}}) = L\cos\theta d\sigma d\Omega, \tag{3.1}$$

where θ is the angle between $\hat{\mathbf{\Omega}}$ and the unit vector $\hat{\mathbf{n}}$ normal to the differential area $d\sigma$.

We can use the radiance to characterize the interaction of the light with the tissue by defining two probability densities: $\mu_a(\hat{\mathbf{\Omega}}, \mathbf{r}, t, \lambda)$ and $p(\hat{\mathbf{\Omega}}, \hat{\mathbf{\Omega}}', \vec{r}, t, \lambda)$. μ_a is the probability density for light absorption in the direction $\hat{\mathbf{\Omega}}$, while p is the probability density of light scattering into the direction $\hat{\mathbf{\Omega}}$ given the incident direction $\hat{\mathbf{\Omega}}'$ at $(\mathbf{r}, t)$.

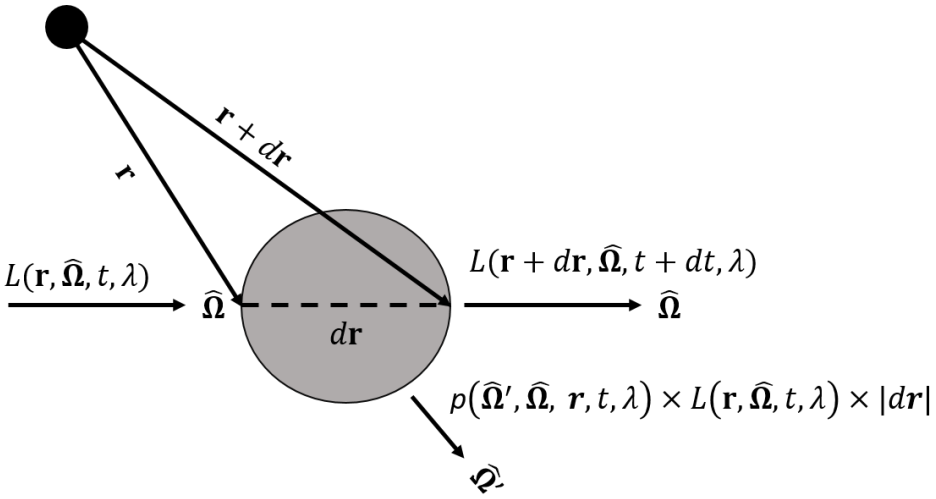

Figure 3.3: Radiance varying after passing through a infinitesimal volume. After traveling a distance $d\mathbf{r}$ in the tissue, L may be absorbed or scattered by the infinitesimal volume. The scattered radiance from direction $\hat{\mathbf{\Omega}}$ to a specific direction $\hat{\mathbf{\Omega}}'$ is proportional to $p(\hat{\mathbf{\Omega}}', \hat{\mathbf{\Omega}}, \mathbf{r}, t, \lambda) \times L(\mathbf{\Omega}, \mathbf{r}, t, \lambda) \times dr$.

With these definitions, the amount of radiance that is absorbed by light propagation through an infinitesimal path, dr, is $\mu_a(\hat{\mathbf{\Omega}}, \mathbf{r}, t, \lambda) \times L \times dr$, while the amount of radiance that is scattered from the direction $\hat{\Omega}$ to the direction $\hat{\Omega}'$ is $p(\hat{\mathbf{\Omega}}', \hat{\mathbf{\Omega}}, \mathbf{r}, t, \lambda) \times L \times |d\mathbf{r}|$, see figure 3.3. Hence, we can integrate the last expression over all solid angles in order to find an expression, called scattering coefficient (μ_s), which accounts for scattering events into all directions of the incident light in the direction $\hat{\mathbf{\Omega}}$.

$$\int_0^{2\pi} \int_0^{\pi} p(\hat{\mathbf{\Omega}}', \hat{\mathbf{\Omega}}, \mathbf{r}, t, \lambda) \times L(\mathbf{\Omega}, \mathbf{r}, t, \lambda) \times dr \times d\Omega' =$$
$$= L(\hat{\mathbf{\Omega}}, \mathbf{r}, t, \lambda) \times dr \times \int_0^{2\pi} \int_0^{\pi} p(\hat{\mathbf{\Omega}}', \hat{\mathbf{\Omega}}, \mathbf{r}, t, \lambda) d\Omega', \tag{3.2}$$

then the amount of radiance that is scattered from the direction $\hat{\mathbf{\Omega}}$ to any other direction is given by:

$$L(\hat{\mathbf{\Omega}}, \mathbf{r}, t, \lambda)\mu_s dr, \tag{3.3}$$

where μ_s is defined as $\int_0^{2\pi} \int_0^{\pi} p(\hat{\mathbf{\Omega}}', \hat{\mathbf{\Omega}}, \mathbf{r}, t, \lambda) d\Omega'$. This coefficient is well-known as the scattering coefficient.

The coefficients μ_a and μ_s have similar meanings; μ_a and μ_s stand to the wavelength-dependent probability for absorption of light in the $\hat{\mathbf{\Omega}}$ direction and scattering of light from the $\hat{\mathbf{\Omega}}$ direction to any other one, respectively. With the aforementioned coefficients, we can calculate the mean distance a photon travels between two events of

scattering and two events of absorption. First of all, the number of photons that were not scattered after traveling a distance of $r + dr$ is given by:

$$N(r + dr) = N(r) - N(r)\mu_s dr, \tag{3.4}$$

expanding the last side of the equation in Taylor up to the first order:

$$N(r) + \frac{dN}{dr}dr = N(r) - N(r)\mu_s dr, \tag{3.5}$$

then

$$\frac{dN}{N} = -\mu_s dr \rightarrow N(r) = N_0 e^{-\mu_s r}. \tag{3.6}$$

To find the mean distance that a photon propagates through the tissue without scattering, we should realize that two phenomena happen for a photon scattering after a distance r without being scattered before: (1) it did not scatter during a distance r and; (2) it scattered after the distance r. Therefore, the density probability for a photon to scatter after traveling a distance r without scattering should be the density probability of not scattering in the distance r ($\frac{N(r)}{N_0}$) times the probability of scattering ($\mu_s dr$). Hence,

$$< r_s >= \int_0^\infty r\frac{N(r)}{N_0}\mu_s dr = \int_0^\infty re^{(-\mu_s r)}\mu_s dr = \frac{1}{\mu_s}, \tag{3.7}$$

in which the index s refers to scattering. Using the same approach, one can calculate the mean distance that a photon propagates between two events of absorption, finding that $< r_a >= \frac{1}{\mu_a}$.

$< r_s >$ and $< r_a >$ are important for our approach since the RT theory only works for media in which both are significantly greater than the light wavelength. In the NIR spectra, this requirement is acquired, considering the interaction with the biological tissue.

The infinitesimal light radiance change, dL, after passing through an infinitesimal volume is given by:

$$dL = L(\mathbf{r} + d\mathbf{r}, \hat{\mathbf{\Omega}}, t + dt) - L(\mathbf{r}, \hat{\mathbf{\Omega}}, t).$$

Expanding again in Taylor:

$$dL = \frac{\partial L(\mathbf{r}, \hat{\mathbf{\Omega}}, t)}{\partial t}dt + d\mathbf{r} \cdot \nabla L(\mathbf{r}, \hat{\mathbf{\Omega}}, t)$$

but $v = \frac{d\mathbf{r}\cdot\hat{\mathbf{\Omega}}}{dt} \rightarrow d\mathbf{r} = vdt\hat{\mathbf{\Omega}}$. v is the light velocity between interactions. Therefore,

$$dL = \frac{\partial L(\mathbf{r}, \hat{\mathbf{\Omega}}, t)}{\partial t} dt + v dt \hat{\mathbf{\Omega}} \cdot \nabla L(\mathbf{r}, \hat{\mathbf{\Omega}}, t). \tag{3.8}$$

Moreover, we can also construct another and equivalent expression to dL based on μ_a and p:

$$dL = -\mu_a(\hat{\mathbf{\Omega}}, \mathbf{r}, t) L(\mathbf{r}, \hat{\mathbf{\Omega}}, r) dr - L(\mathbf{r}, \hat{\mathbf{\Omega}}, r) \int_{\hat{\mathbf{\Omega}} \neq \hat{\mathbf{\Omega}}'} p(\hat{\mathbf{\Omega}}', \hat{\mathbf{\Omega}}, \mathbf{r}, t) d\hat{\mathbf{\Omega}}' dr +$$

$$\int_{\hat{\mathbf{\Omega}} \neq \hat{\mathbf{\Omega}}'} p(\hat{\mathbf{\Omega}}, \hat{\mathbf{\Omega}}', \mathbf{r}, t) L(\mathbf{r}, \hat{\mathbf{\Omega}}', r) d\hat{\mathbf{\Omega}}' dr + Q(\mathbf{r}, \hat{\mathbf{\Omega}}, t, \lambda) dr. \tag{3.9}$$

To clarify, in equation 3.9, the first term corresponds to the radiance that is absorbed by the media in the direction $\hat{\mathbf{\Omega}}$. The second and third terms stand to the radiance that are scattered to a different direction $\hat{\mathbf{\Omega}}$ and from any other direction $\hat{\mathbf{\Omega}}'$ to the direction $\hat{\mathbf{\Omega}}$, respectively. Finally, the last term accounts for light sources that emit power per unit volume at position $\mathbf{r}$ and time t in the direction $\hat{\mathbf{\Omega}}$. If we take a careful look again in the equation 3.3, we can see that μ_s is defined by integrating the second term of equation 3.9 over all solid angles. Therefore, by adding $-p(\hat{\mathbf{\Omega}}, \hat{\mathbf{\Omega}}, \mathbf{r}, t, \lambda) L(\mathbf{r}, \hat{\mathbf{\Omega}}', r) dr + p(\hat{\mathbf{\Omega}}, \hat{\mathbf{\Omega}}, \mathbf{r}, t, \lambda) L(\mathbf{r}, \hat{\mathbf{\Omega}}', r) dr$, which is zero, we will have:

$$dL = -\mu_a(\hat{\mathbf{\Omega}}, \mathbf{r}, t) L(\mathbf{r}, \hat{\mathbf{\Omega}}, t) dr - L(\mathbf{r}, \hat{\mathbf{\Omega}}, t) dr \int_{4\pi} p(\hat{\mathbf{\Omega}}', \hat{\mathbf{\Omega}}, \mathbf{r}, t) d\hat{\mathbf{\Omega}}'$$

$$\int_{4\pi} p(\hat{\mathbf{\Omega}}, \hat{\mathbf{\Omega}}', \mathbf{r}, t) L(\mathbf{r}, \hat{\mathbf{\Omega}}', t) d\hat{\mathbf{\Omega}}' dr + Q(\mathbf{r}, \hat{\mathbf{\Omega}}, t, \lambda) dr;$$

changing dr by vdt and using the definition of μ_s,

$$dL = -\mu_a(\hat{\mathbf{\Omega}}, \mathbf{r}, t) L(\mathbf{r}, \hat{\mathbf{\Omega}}, t) v dt - L(\mathbf{r}, \hat{\mathbf{\Omega}}, t) \mu_s(\hat{\mathbf{\Omega}}, \mathbf{r}, t) v dt +$$

$$+ \int_{4\pi} p(\hat{\mathbf{\Omega}}, \hat{\mathbf{\Omega}}', \mathbf{r}, t) L(\mathbf{r}, \hat{\mathbf{\Omega}}', t) d\hat{\mathbf{\Omega}}' v dt + Q(\mathbf{r}, \hat{\mathbf{\Omega}}, t, \lambda) v dt, \tag{3.10}$$

Finally, combining equations 3.8 and 3.10, we have:

$$\frac{\partial L(\mathbf{r}, \hat{\mathbf{\Omega}}, t)}{\partial t} dt + v dt \hat{\mathbf{\Omega}} \cdot \nabla L(\mathbf{r}, \hat{\mathbf{\Omega}}, t) = -\left[\mu_a(\hat{\mathbf{\Omega}}, \mathbf{r}, t) + \mu_s(\hat{\mathbf{\Omega}}, \mathbf{r}, t)\right] L(\mathbf{r}, \hat{\mathbf{\Omega}}, t) v dt +$$

$$+ \int_{4\pi} p(\hat{\mathbf{\Omega}}, \hat{\mathbf{\Omega}}', \mathbf{r}, t) L(\mathbf{r}, \hat{\mathbf{\Omega}}', t) d\hat{\mathbf{\Omega}}' v dt + Q(\mathbf{r}, \hat{\mathbf{\Omega}}, t, \lambda) v dt, \tag{3.11}$$

dividing both sides by vdt:

$$\frac{1}{v}\frac{\partial L(\mathbf{r},\hat{\mathbf{\Omega}},t)}{\partial t}+\hat{\mathbf{\Omega}}\cdot\nabla L(\mathbf{r},\hat{\mathbf{\Omega}},t)=-\Big[\mu_a(\hat{\mathbf{\Omega}},\mathbf{r},t)+\mu_s(\hat{\mathbf{\Omega}},\mathbf{r},t)\Big]\,L(\mathbf{r},\hat{\mathbf{\Omega}},t)+$$

$$+\int_{4\pi}p(\hat{\mathbf{\Omega}},\hat{\mathbf{\Omega}}',\mathbf{r},t)L(\mathbf{r},\hat{\mathbf{\Omega}}',t)d\hat{\mathbf{\Omega}}'+Q(\mathbf{r},\hat{\mathbf{\Omega}},t,\lambda). \tag{3.12}$$

Equation 3.12 is the well-known radiative transport equation (RTE). However, it is not in the most common form. To express it in the commonly used form, we should define the total transport coefficient, $\mu_t \equiv \mu_a(\hat{\mathbf{\Omega}},\mathbf{r},t)+\mu_s(\hat{\mathbf{\Omega}},\mathbf{r},t)$, and the normalized scattering phase function,$f \equiv \frac{p(\hat{\mathbf{\Omega}},\hat{\mathbf{\Omega}}',\mathbf{r},t,\lambda)}{\mu_s(\hat{\mathbf{\Omega}},\mathbf{r},t,\lambda)}$. Hence,

$$\frac{1}{v}\frac{\partial L(\mathbf{r},\hat{\mathbf{\Omega}},t)}{\partial t}=-\hat{\mathbf{\Omega}}\cdot\nabla L(\mathbf{r},\hat{\mathbf{\Omega}},t)-\mu_t(\hat{\mathbf{\Omega}},\mathbf{r},t,\lambda)L(\mathbf{r},\hat{\mathbf{\Omega}},t)+$$

$$+Q(\mathbf{r},\hat{\mathbf{\Omega}},t,\lambda)+\mu_s(\hat{\mathbf{\Omega}},\mathbf{r},t,\lambda)\int_{4\pi}f(\hat{\mathbf{\Omega}},\hat{\mathbf{\Omega}}',\mathbf{r},t,\lambda)L(\mathbf{r},\hat{\mathbf{\Omega}}',t)d\hat{\mathbf{\Omega}}'. \tag{3.13}$$

RTE is the main result of this section, and it is important to note that to derive this equation, we only defined the radiance as the light power per unit area per unit solid angle traveling a specific direction. Next, we investigated its interaction with the medium, considering the capability of tissue to absorb and scatter radiance, or light. Another important note is that our derivation of the RTE considers only unpolarized light. Otherwise, we would have to use absorption and scattering coefficients that accounts for each direction of polarization. In that case, the radiance L should be replaced by a 4×1 vector, and we would have to replace μ_s, μ_a and p by 4×4 tensors [15].

The radiative transport equation is an approximation to the Maxwell's equations to the propagation of light through the tissue. However, the equation 3.13 is only analytically solvable for very simple geometries which is not the case at hand. In the case of NIR light and biological tissue, we can still approximate the 3.13 by a diffusive process under some assumptions that will be discussed in the next section.

3.3 Photon Diffusive Approximation

In this section, we will find an approximation to the RTE by: (1) finding the continuity relation between photon fluence and flux and; (2) expanding the radiance in spherical harmonics up to the first order. Dividing $L(\mathbf{r},\hat{\mathbf{\Omega}},t)$ by v in which v is the velocity of light between tissue interaction, scattering or absorption, we can make the following dimensional analysis:

$$\frac{L(\mathbf{r},\hat{\mathbf{\Omega}},t)}{v} = \frac{[Wcm^{-2}sr^{-1}]}{[cmt^{-1}]} = \frac{[Wsr^{-1}]\times[t]}{[cm^3]} = \frac{[Energy][sr^{-1}]}{[Volume]}. \tag{3.14}$$

Therefore, $\frac{L(\mathbf{r},\hat{\mathbf{\Omega}},t)}{v}$ is basically the component of the photon energy concentration ($Energy/volume$) traveling in the $\hat{\mathbf{\Omega}}$ direction. To find the total photon energy concentration, denoted by $\Gamma(\mathbf{r},t)$, we can integrate L/v over all solid angles. Thus,

$$\Gamma(\mathbf{r},t) = \frac{1}{v}\int_{4\pi} L(\mathbf{r},\hat{\mathbf{\Omega}},t)d\Omega = \frac{1}{v}\Phi(\mathbf{r},t), \tag{3.15}$$

where $\Phi(\mathbf{r},t) = \frac{[W]}{cm^{-2}}$ is the photon fluence rate. With the definition of the photon fluence rate, we can come back to equation 3.13 and integrate it in both sides over all solid angles. Hence,

$$\frac{1}{v}\frac{\partial}{\partial t}\int_{4\pi} L(\mathbf{r},\hat{\mathbf{\Omega}},t)d\Omega = -\int_{4\pi}\nabla\cdot[L(\mathbf{r},\hat{\mathbf{\Omega}},t)\hat{\mathbf{\Omega}}]d\Omega - \int_{4\pi}\mu_t(\hat{\mathbf{\Omega}},\mathbf{r},t,\lambda)L(\mathbf{r},\hat{\mathbf{\Omega}},t)d\Omega +$$

$$+\int_{4\pi} Q(\mathbf{r},\hat{\mathbf{\Omega}},t,\lambda)d\Omega + \int_{4\pi}\mu_s(\hat{\mathbf{\Omega}},\mathbf{r},t,\lambda)\int_{4\pi} f(\hat{\mathbf{\Omega}},\hat{\mathbf{\Omega}}',\mathbf{r},t,\lambda)L(\mathbf{r},\hat{\mathbf{\Omega}}',t)d\Omega'd\Omega. \tag{3.16}$$

Now, if we assume that the medium is isotropic, i.e. the scattering and the absorption coefficients do not depend on the direction of light, the gradient of L in spherical coordinates, μ_s and μ_a, become:

$$\nabla L = \frac{\partial L}{\partial r}\hat{\mathbf{r}} + \frac{1}{r}\frac{\partial L}{\partial r}\hat{\theta} + \frac{1}{r\sin\theta}\frac{\partial L}{\partial r}\hat{\phi} \to \frac{\partial L}{\partial r}\hat{\mathbf{r}},$$

$$\mu_s(\hat{\mathbf{\Omega}},\mathbf{r},t,\lambda) \to \mu_s(\mathbf{r},t,\lambda), \text{ and}$$

$$\mu_a(\hat{\mathbf{\Omega}},\mathbf{r},t,\lambda) \to \mu_a(\mathbf{r},t,\lambda).$$

From now on, I will omit the dependence on the wavelength λ for simplicity of notation. Therefore,

$$\frac{1}{v}\frac{\partial\Phi(\mathbf{r},t)}{\partial t} = -\nabla\cdot\int_{4\pi} L(\mathbf{r},\hat{\mathbf{\Omega}},t)\hat{\mathbf{\Omega}}d\Omega - \mu_t(\mathbf{r},t)\Phi(\mathbf{r},t) +$$

$$+ S(\mathbf{r},t) + \mu_s(\mathbf{r},t)\int_{4\pi}\int_{4\pi} f(\hat{\mathbf{\Omega}},\hat{\mathbf{\Omega}}',\mathbf{r},t)L(\mathbf{r},\hat{\mathbf{\Omega}}',t)d\Omega'd\Omega; \tag{3.17}$$

where $S(\mathbf{r},t)$ is the concentration of an arbritary radiant source power. It has units of $[W/cm^{-3}]$. Further, we can assume that the scattering phase function (f) depends only on the angle between the incident and scattered wave vectors, i.e.

$$f(\hat{\mathbf{\Omega}},\hat{\mathbf{\Omega}}',\mathbf{r},t) = f(\hat{\mathbf{\Omega}}\cdot\hat{\mathbf{\Omega}}',\mathbf{r},t),$$

then

$$\frac{1}{v}\frac{\partial\Phi(\mathbf{r},t)}{\partial t} = -\nabla\cdot\int_{4\pi} L(\mathbf{r},\hat{\mathbf{\Omega}},t)\hat{\mathbf{\Omega}}d\Omega - \mu_t(\mathbf{r},t)\Phi(\mathbf{r},t)+$$

$$+S(\mathbf{r},t) + \mu_s(\mathbf{r},t,\lambda)\int_{4\pi}\left\{\int_{4\pi} f(\hat{\mathbf{\Omega}}\cdot\hat{\mathbf{\Omega}}',\mathbf{r},t)d\Omega\right\} L(\mathbf{r},\hat{\mathbf{\Omega}}',t)d\Omega'.$$

Where

$$\int_{4\pi} f(\hat{\mathbf{\Omega}}\cdot\hat{\mathbf{\Omega}}',\mathbf{r},t)d\Omega = 1.$$

Thus,

$$\frac{1}{v}\frac{\partial\Phi(\mathbf{r},t)}{\partial t} = -\nabla\cdot\int_{4\pi} L(\mathbf{r},\hat{\mathbf{\Omega}},t)\hat{\mathbf{\Omega}}d\Omega - \mu_a(\mathbf{r},t)\Phi(\mathbf{r},t) + S(\mathbf{r},t).$$

Defining the photon flux as

$$\mathbf{J}(\mathbf{r},t) = \int_{4\pi} L(\mathbf{r},\hat{\mathbf{\Omega}},t)\hat{\mathbf{\Omega}}d\Omega, \tag{3.18}$$

we have the continuity relation between the photon fluence rate and the photon flux, which is given by:

$$\frac{1}{v}\frac{\partial\Phi(\mathbf{r},t)}{\partial t} + \nabla\cdot\mathbf{J}(\mathbf{r},t) + \mu_a(\mathbf{r},t,\lambda)\Phi(\mathbf{r},t) = S(\mathbf{r},t,\lambda). \tag{3.19}$$

Note that there is a crucial difference between the fluence rate, $\Phi(\mathbf{r},t)$, and the photon flux, $\mathbf{J}(\mathbf{r},t)$. $\Phi(\mathbf{r},t)$ is the scalar sum over all angles of the radiance emerging from the infinitesimal volume centered at $(\mathbf{r},t)$, while $\mathbf{J}(\mathbf{r},t)$ is the vector sum of the radiance over all angles. For example, for an incandescent light bulb, $\Phi(\mathbf{r},t)$ is much larger than $||\mathbf{J}(\mathbf{r},t)||$ (Figure 3.4a), while for a colimated laser both are approximately the same (Figure 3.4b) since in the first case the light propagates approximately equally over all directions and in the second it travels mostly over one direction.

(a) Incandescent light bulb

(b) Colimated Laser

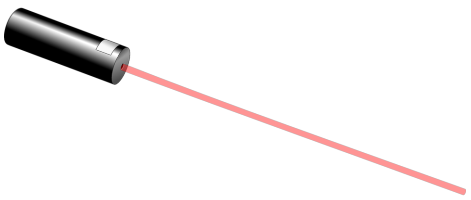

Figure 3.4: Example of two sources to illustrate the intrinsic difference between photon fluence rate and photon flux. The photon fluence rate is defined as the scalar sum over all solid angles of radiance emerging radially from a infinitesimal volume, while the photon flux is the vector sum. For an incandescent light, $||\mathbf{J}(\mathbf{r},t)|| \to 0$, and for a laser $||\mathbf{J}(\mathbf{r},t)|| \sim \Phi(\mathbf{r},t)$.

3.3.1 Spherical Harmonics Expansion of the Light Radiance

The next step to find the diffuse approximation to the RTE is to expand the light radiance L as a series of spherical harmonics, Y_l^m. Before doing that, let us remember some properties of spherical harmonics and some mathematical relations that will be useful.

1. $f(\theta,\phi) = \sum_{l=0}^{\infty}\sum_{m=-l}^{+l}\sqrt{\frac{2l+1}{4\pi}}f_l^m Y_l^m(\theta,\phi)$. Spherical harmonics expansion series.
2. $\frac{2l+1}{4\pi}\int_{4\pi} Y_l^m Y_{l'}^{m'} d\Omega = \delta_{ll'}\delta_{mm'}$. Ortogonality.
3. $\hat{\mathbf{\Omega}} = \sin\theta\cos\phi\hat{x} + \sin\theta\sin\phi\hat{y} + \cos\theta\hat{z}$. Unit vector in cartesian coordinates.
4. $\int_{4\pi}\hat{\mathbf{\Omega}}(\hat{\mathbf{\Omega}}\cdot\mathbf{A})d\Omega = \frac{4\pi}{3}\mathbf{A}$ and $\int_{4\pi}\hat{\mathbf{\Omega}}[\hat{\mathbf{\Omega}}\cdot\nabla(\mathbf{A}\cdot\hat{\mathbf{\Omega}})]d\Omega = 0$. For any vector $\mathbf{A}$.

With property 1, we can write the light radiance as:

$$L(\mathbf{r},\hat{\mathbf{\Omega}},t) = \sum_{l=0}^{\infty}\sum_{m=-l}^{+l}\sqrt{\frac{2l+1}{4\pi}}f_l^m(\mathbf{r},t)Y_l^m(\theta,\phi), \tag{3.20}$$

substituiting equation 3.20 into the definition of the photon fluence rate:

$$\Phi(\mathbf{r},t) = \int_{4\pi} L(\mathbf{r},\hat{\mathbf{\Omega}},t)d\Omega = \sum_{l=0}^{\infty}\sum_{m=-l}^{+l}\sqrt{\frac{2l+1}{4\pi}}f_l^m(\mathbf{r},t)\int_{4\pi} Y_l^m(\theta,\phi)d\Omega; \tag{3.21}$$

$$\Phi(\mathbf{r},t)=\sum_{l=0}^{\infty}\sum_{m=-l}^{+l}\sqrt{2l+1}f_l^m(\mathbf{r},t)\int_{4\pi}\frac{1}{4\pi}Y_l^m(\theta,\phi)d\Omega, \tag{3.22}$$

but $Y_0^0=\frac{1}{\sqrt{4\pi}}$ then

$$\Phi(\mathbf{r},t)=\sum_{l=0}^{\infty}\sum_{m=-l}^{+l}\sqrt{2l+1}f_l^m(\mathbf{r},t)\int_{4\pi}Y_0^{0*}Y_l^m(\theta,\phi)d\Omega. \text{ For property 2:}$$

$$\Phi(\mathbf{r},t)=f_0^0(\mathbf{r},t). \tag{3.23}$$

We can also expand the photon flux by the same way.

$$\mathbf{J}(\mathbf{r},t)=\int_{4\pi}L(\mathbf{r},\hat{\mathbf{\Omega}},t)\hat{\mathbf{\Omega}}d\Omega=\sum_{l=0}^{\infty}\sum_{m=-l}^{+l}\sqrt{\frac{2l+1}{4\pi}}f_l^m(\mathbf{r},t)\int_{4\pi}Y_l^m(\theta,\phi)\hat{\mathbf{\Omega}}d\Omega=$$

$$=\sum_{l=0}^{\infty}\sum_{m=-l}^{+l}\sqrt{\frac{2l+1}{4\pi}}f_l^m(\mathbf{r},t)\int_{4\pi}Y_l^m(\theta,\phi)[\sin\theta\cos\phi\hat{x}+\sin\theta\sin\phi\hat{y}+\cos\theta\hat{z}]d\Omega=$$

$$\sum_{l=0}^{\infty}\sum_{m=-l}^{+l}\sqrt{\frac{2l+1}{4\pi}}f_l^m(\mathbf{r},t)\int_{4\pi}Y_l^m(\theta,\phi)[\sqrt{\frac{2\pi}{3}}(Y_1^{-1*}-Y_1^{1*})\hat{x}-i\sqrt{\frac{2\pi}{3}}(Y_1^{-1*}+Y_1^{1*})\hat{y}+2\sqrt{\frac{\pi}{3}}Y_1^{0*}\hat{z}].$$

In the last equation, I used property 3 and the definition of Y_1^{-1}, Y_1^1, and Y_1^0. Using again property 2, the photon flux can be written as:

$$\mathbf{J}(\mathbf{r},t)=\sqrt{\frac{1}{2}}\left\{f_1^{-1}(\mathbf{r},t)-f_1^1(\mathbf{r},t)\right\}\hat{x}-i\left\{f_1^{-1}(\mathbf{r},t)+f_1^1(\mathbf{r},t)\right\}\hat{y}+f_1^0(\mathbf{r},t)\hat{z}. \tag{3.24}$$

Now, we can express the net power per area traveling in the $\hat{\mathbf{\Omega}}$ by projecting $\mathbf{J}(\mathbf{r},t)$, i.e. computing the scalar product between $\mathbf{J}(\mathbf{r},t)$ and $\hat{\mathbf{\Omega}}$. Hence,

$$\mathbf{J}(\mathbf{r},t)\cdot\hat{\mathbf{\Omega}}=\sqrt{\frac{4\pi}{3}}\left\{f_1^0(\mathbf{r},t)Y_1^0+f_1^{-1}(\mathbf{r},t)Y_1^{-1}+f_1^1(\mathbf{r},t)Y_1^1\right\}. \tag{3.25}$$

It has been argued in the literature that for the diffuse approximation, L can be expanded up to the first order in the spherical harmonics series [1, 16]. It is known as the P_1 approximation. Therefore,

$$L(\mathbf{r},\hat{\mathbf{\Omega}},t)=\sqrt{\frac{1}{4\pi}}f_0^0(\mathbf{r},t)Y_0^0+\sqrt{\frac{3}{4\pi}}[f_1^{-1}(\mathbf{r},t)Y_1^{-1}+f_1^0(\mathbf{r},t)Y_1^0+f_1^1(\mathbf{r},t)Y_1^1]. \tag{3.26}$$

With equations 3.23, 3.25, and 3.26, we can conclude that P_1 is a linear combination of the photon fluence rate and the photon flux.

$$L(\mathbf{r}, \hat{\mathbf{\Omega}}, t) = \frac{1}{4\pi}\Phi(\mathbf{r}, t) + \frac{3}{4\pi}\mathbf{J}(\mathbf{r}, t) \cdot \hat{\mathbf{\Omega}}. \tag{3.27}$$

If we substitute equation 3.27 in the radiative transport equation 3.13 given by:

$$\frac{1}{v}\frac{\partial L(\mathbf{r}, \hat{\mathbf{\Omega}}, t)}{\partial t} = -\hat{\mathbf{\Omega}} \cdot \nabla L(\mathbf{r}, \hat{\mathbf{\Omega}}, t) - \mu_t(\mathbf{r}, t)L(\mathbf{r}, \hat{\mathbf{\Omega}}, t) +$$

$$+Q(\mathbf{r}, \hat{\mathbf{\Omega}}, t) + \mu_s(\mathbf{r}, t)\int_{4\pi} f(\hat{\mathbf{\Omega}} \cdot \hat{\mathbf{\Omega}}', \mathbf{r}, t)L(\mathbf{r}, \hat{\mathbf{\Omega}}', t)d\hat{\mathbf{\Omega}}',$$

we will have:

$$\frac{1}{v}\frac{\partial}{\partial t}[\frac{1}{4\pi}\Phi(\mathbf{r}, t) + \frac{3}{4\pi}\mathbf{J}(\mathbf{r}, t) \cdot \hat{\mathbf{\Omega}}] = -\hat{\mathbf{\Omega}} \cdot \nabla[\frac{1}{4\pi}\Phi(\mathbf{r}, t) + \frac{3}{4\pi}\mathbf{J}(\mathbf{r}, t) \cdot \hat{\mathbf{\Omega}}] +$$

$$-\mu_t(\hat{\mathbf{\Omega}}, \mathbf{r}, t)[\frac{1}{4\pi}\Phi(\mathbf{r}, t) + \frac{3}{4\pi}\mathbf{J}(\mathbf{r}, t) \cdot \hat{\mathbf{\Omega}}] + Q(\mathbf{r}, \hat{\mathbf{\Omega}}, t) +$$

$$+ \mu_s(\hat{\mathbf{\Omega}}, \mathbf{r}, t)\int_{4\pi} f(\hat{\mathbf{\Omega}} \cdot \hat{\mathbf{\Omega}}', \mathbf{r}, t)[\frac{1}{4\pi}\Phi(\mathbf{r}, t) + \frac{3}{4\pi}\mathbf{J}(\mathbf{r}, t) \cdot \hat{\mathbf{\Omega}}']d\hat{\Omega}', \tag{3.28}$$

The last term can be evaluated defining the direction of $\hat{\mathbf{\Omega}}$ to be $\hat{z}$ so that $\hat{\mathbf{\Omega}}' \cdot \hat{\mathbf{\Omega}} = \cos\theta'$. Therefore,

$$\int_{4\pi} f(\cos\theta')[\frac{1}{4\pi}\Phi + \frac{3}{4\pi}\mathbf{J} \cdot \hat{\mathbf{\Omega}}']d\hat{\Omega}' = \frac{1}{4\pi}\Phi\int_{4\pi} f(\cos\theta')d\hat{\Omega}' +$$

$$+ \frac{3}{4\pi}\int_{4\pi} f(\cos\theta')[\sin\theta'\cos\phi'\hat{x} + \sin\theta'\sin\phi'\hat{y} + \cos\theta'\hat{z}]d\hat{\Omega}'\mathbf{J}, \tag{3.29}$$

but $\int_{4\pi} f(\cos\theta')d\hat{\Omega}' = 1$ and $\int_0^{2\pi}\cos\phi' d\phi' = 0$. Consequently,

$$\int_{4\pi} f(\cos\theta')[\sin\theta'\cos\phi'\hat{x} + \sin\theta'\sin\phi'\hat{y} + \cos\theta'\hat{z}]d\hat{\Omega}'\mathbf{J} = \int_{4\pi} f(\cos\theta')\cos\theta' d\hat{\Omega}'\hat{z} \cdot \mathbf{J} =$$

$$\int_{4\pi} f(\cos\theta')\hat{\mathbf{\Omega}}' \cdot \hat{\mathbf{\Omega}}d\hat{\Omega}'\hat{\mathbf{\Omega}} \cdot \mathbf{J} = g\hat{\mathbf{\Omega}} \cdot \mathbf{J}$$

in which

$$g = \int_{4\pi} f(\cos\theta')\hat{\mathbf{\Omega}}' \cdot \hat{\mathbf{\Omega}}d\hat{\Omega}' = <\cos\theta>. \tag{3.30}$$

g is the scattering anisotropy factor. For an isotropic light tissue interaction, g is equal to 0.5. The equation 3.28 becomes:

$$\frac{1}{v}\frac{\partial}{\partial t}[\Phi + 3\mathbf{J}\cdot\hat{\mathbf{\Omega}}] = -\hat{\mathbf{\Omega}}\cdot\nabla\Phi + 3\hat{\mathbf{\Omega}}\nabla(\mathbf{J}\cdot\hat{\mathbf{\Omega}}) +$$

$$-3\mu_t\hat{\mathbf{\Omega}}\cdot\mathbf{J} + 4\pi Q(\hat{\mathbf{\Omega}}) - (\mu_t - \mu_s)\Phi + 3\mu_s g\hat{\mathbf{\Omega}}\cdot\mathbf{J}; \tag{3.31}$$

for simplicity, I ommitted the dependence of $(\mathbf{r}, t)$ from μ_t, μ_s, Φ, $\mathbf{J}$, and Q. Multiplying both sides of equation 3.31 by $\hat{\mathbf{\Omega}}$, integrating it over all solid angles and using the mathematical property 4, we have:

$$\nabla\Phi = \frac{-3}{v}\frac{\partial\mathbf{J}}{\partial t} - 3(\mu_t - \mu_s g)\mathbf{J} + 3\int_{4\pi} Q(\hat{\mathbf{\Omega}})\hat{\mathbf{\Omega}}d\Omega. \tag{3.32}$$

Now, supposing that all sources Q are isotropic and that the photon flux varies very slowly with time, we have:

$$Q(\hat{\mathbf{\Omega}}) = Q \rightarrow \int_{4\pi} Q(\hat{\mathbf{\Omega}})\hat{\mathbf{\Omega}}d\Omega = Q\int_{4\pi}\hat{\mathbf{\Omega}}d\Omega = 0, \text{ and}$$

$$\frac{-3}{v}\frac{\partial\mathbf{J}}{\partial t} \sim 0 \text{ then}$$

$$\nabla\Phi = -3(\mu_t - \mu_s g)\mathbf{J} \rightarrow \mathbf{J}(\mathbf{r},\mathbf{t}) = \frac{\nabla\Phi(\mathbf{r},t)}{-3(\mu_t(\mathbf{r},t)_-\mu_s(\mathbf{r},t)g)}. \tag{3.33}$$

Defining the reduced scattering coefficient, $\mu_s' = (1-g)\mu_s$, and the photon diffusion coefficient, $D = \frac{v}{3(\mu_s{}' + \mu_a)}$, we have

$$\mathbf{J}(\mathbf{r},\mathbf{t}) = \frac{-D(\mathbf{r},t)}{v}\nabla\Phi(\mathbf{r},t). \tag{3.34}$$

Finally, replacing $\mathbf{J}(\mathbf{r},\mathbf{t})$ in the continuity equation 3.19, we find the diffusion equation to the photon fluence:

$$\frac{1}{v}\frac{\partial\Phi(\mathbf{r},t)}{\partial t} + \nabla\cdot[\frac{-D(\mathbf{r},t)}{v}\nabla\Phi(\mathbf{r},t)] + \mu_a(\mathbf{r},t,\lambda)\Phi(\mathbf{r},t) = S(\mathbf{r},t,\lambda). \tag{3.35}$$

3.4 Summary

In the present chapter, we investigated the physical process behind NIR light propagation trough the biological tissue. We started our study by discussing fundamental concepts of light-matter interaction: scattering and absorption. Next, we chose to model light propagation by using the radiative transport theory, which is an approximation to the Maxwell's equations. In the end of the last section 3.3, we found the photon diffusive approximation to the photon fluence through the biological tissue. It is important to highlight that we had to make several assumptions regarding the nature of light transport. These assumptions are the meaningful physical aspects of this chapter because they assure the validity of the diffusive photon fluence equation. The validity of our findings are assured under:

- **Radiative transport theory works.** The radiative transport equation 3.13 can be applied to model light propagation in which both $< r_s >$ and $< r_a >$ are significantly greater than the light wavelength. In the NIR spectra, this requirement is acquired, considering the interaction with the biological tissue.

- **The scattering and absorption coefficients do not depend on the direction of the light.** To derive the continuity relation between photon fluence rate and photon flux (equation 3.19), we supposed that the medium was isotropic. It means that there is no direction in which light is more scattered or absorbed by the tissue.

- **The normalized phase function depends only on the angle between the incident and scattered wave vectors.** This assumption was also made to derive equation 3.19. The physical meaning of it is that the change on the light direction does not depend on the incident wave-vector.

- **The light radiance can be satisfactorily expanded up to the first order of spherical harmonic series.** If the light radiance is not isotropic after some scattering events it will become at least nearly isotropic. Therefore, the P_1 approximation works properly for systems in which the scattering coefficient is much greater than the absorption coefficient.

- **The photon fluence varies slowly with time.** It implies that the light radiance as a function of time does not change abruptly. In other words, the light radiance interaction with the tissue is stable over time.

Chapter 4

Conclusions

In this work, we discussed the physical principles behind two neuroimaging techniques, nuclear magnetic resonance imaging and near-infrared spectroscopy. Our main goal in this work was to provide a didactic material that could be helpful for new researchers to the neuroscience field and that could be understood by any student in the last year of a physics major.

Chapter 2 is dedicated to the study of nuclear magnetic resonance imaging. By introducing and briefly discussing the concept of nuclear spin, we could model the interactions of hydrogen atoms, or protons, subjected to an external and constant magnetic field and being excited by electromagnetic waves in the radio frequency. We observed that the nuclear magnetic resonance technique is only sensitive to protons on the fundamental states. This is the only mechanism capable to explain why stronger external magnetic fields can provide images with higher contrast and spatial resolution. As the external magnetic field increases, the ratio between protons in the fundamental and excited states also increases.

In addition, we analyzed the effect of applying an oscillating magnetic field to a system of spins under the influence of an external magnetic field. One of our main findings is that to properly model such system, we also had to take into account the thermal equilibrium between the spin lattice and its surroundings. We inferred that magnetic energy were converted to other degrees of freedom of the spin lattice. This process of nonradiative transitions are called *spin-lattice relaxation*. In the last section from chapter 2, we used a phenomenological approach to derive the Bloch equations. To do so, we used the concept of net magnetization, which is the sum of the individual magnetic moments of each proton within a macroscopic volume. With these equations, we could investigate the impact of applying a radio frequency oscillating field to a macroscopic sample of spins. As a result, we could provide physical insights to the longitudinal and transverse spin relaxation times.

In Chapter 3, we investigated the physical principles behind near-infrared light propagation through the biological tissue. We started by discussing scattering and absorption. We argued that under the circumstances of NIRS, we could restrict ourselves to study only elastic scattering, which is characterized by energy conservation of the scattered photon. We also discoursed in which conditions an incident photon could be absorbed by the biological tissue.

Next, we used the Radiative Transport (RT) Theory as an approximation to Maxwell's equations for describing light propagation through tissue. By using the concept of light radiance and defining two probability densities related to absorption and scattering, we could model the light propagation and derive the Radiative Transport equation. By making several reasonable assumptions regarding the nature of light transport, we found that NIR light propagation in the biological tissue could be modeled by a photon diffusive equation.

The validity of our findings in Chapter 3 are assured under several conditions. First, the mean path between two events of scattering and absorption must be significantly higher than the light wavelength. Second, the scattering and absorption coefficients do not depend on the directions of the light, which implies that the medium is isotropic. Third, the change in the direction of light due to scattering do not depend on the incident wave-vector. Fourth, the light radiance is nearly isotropic, which means that the scattering coefficient is much greater than the absorption coefficient. Finally, the light radiance as a function of time does not change abruptly. Under these conditions, it is possible to estimate absorption and scattering coefficients from the diffuse equation and monitor their changes in biological tissue.

Bibliography

[1] W. B. Baker, *Optical Cerebral Blood Flow Monitoring of Mice to Men.* PhD thesis, University of Pennsylvania, 2015.

[2] E. J. Sanz-Arigita, M. M. Schoonheim, J. S. Damoiseaux3, S. A. R. B. Rombouts, E. Maris, F. Barkhof, P. Scheltens, and C. J. Stam, "Loss of small-world networks in alzheimers disease: Graph analysis of fmri resting-state functional connectivity," *Plos One*, vol. 5, pp. 1–14, 2010.

[3] C. Lin Yasuda, Z. Chen, G. Coco Beltramini, A. C. Coan, M. E. Morita, B. Kubota, F. Bergo, C. Beaulieu, F. Cendes, and D. William Gross, "Aberrant topological patterns of brain structural network in temporal lobe epilepsy," *Epilepsia*, vol. 56, pp. 1992–2002, 2015.

[4] F. L. da Silva, "Eeg: Origin and measurement," *EEG fMRI*, pp. 19–38, 2010.

[5] G. C. Beltramini, *Análise temporal de correlatos hemodinâmicos associados à atividade epileptiforme através da técnica de EEG-RMf simultâneos.* PhD thesis, University of Campinas, 2014.

[6] A. Villringer and C. B., "Non-invasive optical spectroscopy and imaging of human brain function," *Trends Neurosic*, vol. 20, pp. 435–442, 1997.

[7] A. Yodh and D. Boas, "Functional imaging with diffusing light," pp. 435–442, 2003.

[8] Y. Fukui, Y. Ajichi, and E. Okada, "Monte carlo prediction of near-infrared light propagation in realistic adult and neonatal head models," *Applied Optics*, vol. 42, pp. 2881–2887, 2003.

[9] C. Tannoudjj, *Quantum Mechanics.* Hermann and John Wiley, 1977.

[10] F. Bloch, "Nuclear introduction," *Physical Review*, vol. 70, pp. 460–473, 1946.

[11] S. Chandrasekhar, *Radiative Transfer*. Dover, 1960.

[12] A. Ishimaru, *Wave Propagation and Scattering in Random Media*. Academic Press, Inc San Diego, 1978.

[13] J. Ripoll, "Derivation of the scalar radiative transfer equation from energy conservation of maxwell's equations in the far field," *J. Opt. Soc. Am. A*, vol. 28, pp. 1765–1775, Aug 2011.

[14] R. C. Mesquita and A. G. Yodh, "Diffuse optics: Fundamentals and tissue applications," 2011.

[15] M. I. Mishchenko, "Poyntingstokes tensor and radiative transfer in discrete random media: The microphysical paradigm," *Opt. Express*, vol. 18, pp. 1765–1775, 2010.

[16] R. C. Mesquita, *Desenvolvimento de métodos ópticos para o estudo do acoplamento neuro-vascular-metabólico intrínseco à dinâmica cerebral*. PhD thesis, University of Campinas, 2009.